buildings

MDPI

Article

Effects of Fly Ash Composition to Mitigate Conversion of Calcium Aluminate Cement Composites

Thwe Thwe Win [1], Chinnapat Panwisawas [2], Pitcha Jongvivatsakul [3], Withit Pansuk [3] and Lapyote Prasittisopin [1,*]

[1] Architectural Technology Research Unit, Department of Architecture, Faculty of Architecture, Chulalongkorn University, Bangkok 10330, Thailand
[2] School of Engineering and Materials Science, Queen Mary University of London, London E1 4NS, UK
[3] Centre of Excellence in Innovative Construction Materials, Department of Civil Engineering, Faculty of Engineering, Chulalongkorn University, Bangkok 10330, Thailand
* Correspondence: lapyote.p@chula.ac.th

Abstract: Calcium aluminate cement (CAC) is one of the alternative cements that is widely used for special applications. However, during the hydration process degradation of CAC microstructure, the so-called hydrate conversion process, hexagonal calcium aluminate hydrate (CAH_{10}) transforms into a cubic (C_3AH_6) phase, resulting in increased porosity and reduced strengths. It is known that alternative means for stabilizing the CAC conversion are conducted by introducing fly ash (FA) in CAC, where its microstructure is attributed to aluminosilicates. However, no study has yet been conducted on different FA compositions influencing CAC performance. This study aims to evaluate the effects of different compositions of FA on CACs' fresh and hardened characteristics. Results revealed that the microstructure was denser when CAC was mixed with FA. Regarding reactivity, CAC with calcium-rich FA systems is 13% faster than the silica-rich one. The higher the density and the lower the porosity of calcium-rich FA mixtures were found compared with silica-rich FA in both micro- and macro-structures. As seen in the microscopic structure, this is due to the calcium-rich phase formation.

Keywords: fly ash; calcium aluminate cement; conversion; hydration; performance; composition

Citation: Win, T.T.; Panwisawas, C.; Jongvivatsakul, P.; Pansuk, W.; Prasittisopin, L. Effects of Fly Ash Composition to Mitigate Conversion of Calcium Aluminate Cement Composites. *Buildings* **2023**, *13*, 2453. https://doi.org/10.3390/buildings13102453

Academic Editor: Tomáš Dvorský

Received: 4 September 2023
Revised: 19 September 2023
Accepted: 22 September 2023
Published: 27 September 2023

1. Introduction

Calcium aluminate cement (CAC) or high-alumina cement is widely used and usually adopted in engineering applications with special purposes, such as refractory, biomaterial, ability to resist acid exposure, fast-setting, durable, and additive manufacturing concretes [1]. Several research programs were being determined, especially for the purposes of property improvement, durability, and more eco-friendly production processes. In addition, during the manufacturing process of CAC, depending on the availability of the source, it is reported that there is a significant reduction in carbon dioxide emissions generated in the atmosphere from lower sintering temperatures compared to portland cement, so CAC can be considered an eco-cement material.

One of the primary applications of CAC is in the construction sector. It is widely used in refractory applications due to its ability to withstand extreme temperatures, making it invaluable in the manufacturing of furnaces, kilns, and foundry linings. Moreover, CAC is employed in high-performance concrete formulations, where its rapid setting and exceptional strength gain are critical, particularly in precast concrete elements and underwater construction [2].

However, the widespread adoption of CAC-based materials is not without challenges. Regulatory constraints governing the use of CAC can vary significantly from one country to another. These constraints may pertain to environmental considerations and quality control

measures. Understanding these variations and how they impact the use of CAC-based materials is essential for engineers and researchers.

One of the primary concerns associated with CAC is the hydrate conversion process during hydration, which can impact the material's performance. The CA phase is the fundamental hydraulic phase in all CAC systems. Regarding the affecting factors, the most significant factor is the curing temperature, since the hydration product directly relies on the curing temperature [3]. CAH_{10} and C_2AH_8 phases are regarded as metastable at ambient temperature [4] and ultimately change to the more stable C_3AH_6 and AH_3 phases due to thermodynamic stabilization. The conversion from the metastable to stable phases leads to porosity gains, more permeability, and hence strength reduction [5]. The conversion reactions are presented in Equations (1) and (2). The hydration reaction of CA produced is dependent on the temperature, which is given in Table 1. The strength progression of CAC concrete at room temperature is shown in Figure 1. The strength first rises rapidly to a high early strength (corresponding to CAH_{10} and C_2AH_8), then gradually drops to a minimum (during the transformation to C_3AH_6 and AH_3) before rising once more from prolonged hydration.

$$2CAH_{10} \longrightarrow C_2AH_8 + AH_3 + 9H \quad (1)$$

$$3C_2AH_8 \longrightarrow 2C_3AH_6 + AH_3 + 9H \quad (2)$$

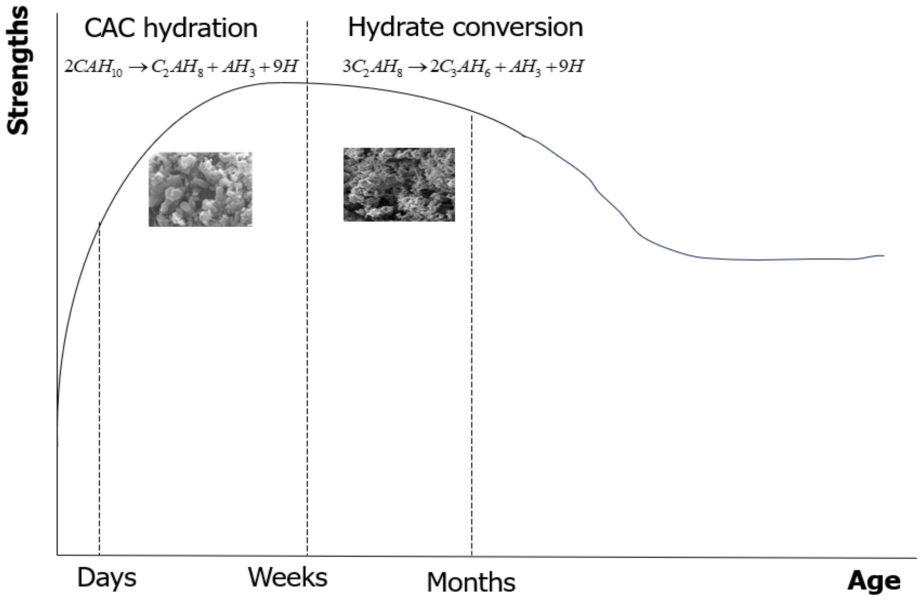

Figure 1. Schematic strength development of CAC concrete at ambient temperature.

Boris et al. [6] investigated the conversion process, especially in the presence of nanomaterials. These nanomaterials vary in chemical composition and grain size, and their effects on CAC depend on their type and quantity. Nano-silica was found to accelerate the CAC hydration process, shortening the induction period and intensifying the secondary heat release effect. Despite similar types of hydration products in all CAC pastes, the quantitative composition could vary [6]. Due to this conversion effect, the implementation of CAC in structural engineering practice is restricted. Although CAC is no longer a novel material, the conversion raises questions about how well it performs under harsh loading and the stability of its microstructure. The processes that transform the metastable phases of CAH_{10} and C_2AH_8 into stable, long-lasting, and dense C_3AH_6 hydrates are responsible for this thermodynamic instability [7,8]. Many researchers have attempted to identify the chemical reactions and the effects of the conversion on the overall performance of CAC concretes [8,9]. Some researchers [3–5] have investigated whether replacing some of the

CAC with pozzolanic materials such as ground granulated blast furnace slag (GGBFS), metakaolin, silica fume, and rice husk ash is a proper technique to mitigate the hydrate conversion process and strength reduction.

Therefore, utilizing coal fly ash (FA) as pozzolan in CAC is carried out to overcome the conversion process. The incorporation of FA could improve the hydrogarnet due to an aluminate hydrate reacting alternatively to silica in the C-A-S-H phase or stratlingite (C_2ASH_8) [2,10] as revealed by the subsequent equations:

$$2CAH_{10} + S \longrightarrow C_2ASH_8 + AH_3 + 9H \quad (3)$$

$$C_2AH_8 + S \longrightarrow C_2ASH_8 \quad (4)$$

Majumdar and Singh [11] found that replacing CAC with pozzolanic materials such as micro-silica, GGBFS, and metakaolin reduced the hydrate conversion while also increasing its strengths. Its hydrate conversion of hexagonal hydrated structures could be prevented by the pozzolanic reaction in the CAC system, which has been observed in the reaction of CA. Lastly, this reaction could prevent hexagonal (C_2AH_8) formation and C_3AH_6 transformation [11,12].

FA is an industrial by-product with very fine particles that is manufactured from the combustion of coal in power plants. FA has a spherical shape that has a high silica and calcium composition [13]. Although the CAC hydration process may receive some attention for inclusion with pozzolanic materials by many researchers, the mechanical and microstructural performances of such systems have not been systematically investigated in engineering applications. In addition, the effect of pozzolanic materials on the hydration reaction of CAC and its mechanical performance have not been completely investigated. Similarly, a study that examines how FA impacts the mechanical and microstructural characteristics of CAC systems is lacking.

Based on the alumina and calcium contents, various CAC systems are remarkably different, with low silica contents. The mechanical properties of this CAC concrete can be changed by variations in the alumina content [14]. Although it has been researched how the water-to-cement ratio (w/c) affects the fracture performance of CAC concrete, the effect of adopting different silica contents in the CAC system has not been reviewed yet [15]. According to the review of the literature, the novelty of this work includes:

- The effect of replacing FA with CAC has not been thoroughly considered.
- The effect of two types of FA (class F and class C) on the performance of this type of cement has not been investigated.

The experiment explores various aspects of CAC composites incorporating FA, entailing initial setting time, evolution of FA reactivity, workability, densities at 7, 28, and 56 days, compressive strengths at 7, 28, and 56 days, and porosities at 7, 28, and 56 days. To examine the pore structures and chemical composition of CAC, including FA, nitrogen adsorption and thermogravimetric analysis (TGA) have been performed. Furthermore, microstructural analysis using Scanning Electron Microscopy (SEM) with Energy Dispersive Spectrometer (EDS) has been employed to gain a deeper understanding of the transformation of CAC containing FA.

Table 1. Summary of the temperature history of conversion reaction of CAC from literature.

Reference	Temperature Range (°C)		
	CAH_{10}	C_2AH_8	C_3AH_6
Scrivener et al. [16]	<15	15–70	>70
Adams et al. [17]	<15	15–27	>27
Khaliq and Khan [18]	<15	15–27	>27
Zapata et al. [19]	<15	15–35	>35

Table 1. *Cont.*

Reference	Temperature Range (°C)		
	CAH_{10}	C_2AH_8	C_3AH_6
Son et al. [20]	<20	20–40	40–60
Antonovič et al. [7]	5	20	40
Ukrainczyk and Matusinović [21]	20	30	>55
Vafaei and Allahverdi [14]	15–25	25–40	40–60
Zapata et al. [9]	≥20	~30	>55
Mean	<16	28	>45
Median	<15	15–27	>40

2. Materials and Methods

2.1. Materials

The CAC used in the preparation of the mixture was Secar 71, manufactured by Kerneos in Paris, France. Standard sand, in accordance with ASTM C33 [22], was utilized as fine aggregate for making CAC mortar. The standard sand, which has a specific gravity of 2.61, a fineness modulus of 2.96, and a water absorption of 0.66%, was obtained from Saraburi Province, Thailand [23]. Deionized water was used throughout the experiment. Two types of as-received FA were procured from different sources. SEM pictures of aluminosilicate sources display that both class F (FA1) and class C FA (FA2) have spherical shapes, and CAC has angular and asymmetrical shapes (in Figure 2). Figure 3 shows the sieve analysis of fine aggregate obtained from the sieve test and the upper and lower limits according to ASTM C33 [22]. Their grading meets the limits specified by ASTM standards. The aggregate was used in this investigation under saturated surface dry (SSD) conditions. It should be mentioned that the used FA was categorized into two types: low calcium content FA (class F, max: 18%) and high calcium content FA (class C > 18%) according to the ASTM C618 specification on pozzolanic materials [24]. FA employed here was supplied for class F and class C FA from sources in Map Ta Phut Industrial Estate, Rayong Province, Thailand, and Mae Moh, Lampang Province, Thailand, respectively. The chemical composition of CAC and FA analyses was performed using X-ray Fluorescence Spectroscopy (XRF) (BRUKER S8 TIGER instrument, Bruker Corporation, Bremen, Germany). In addition, the Blaine-specific surface areas of CAC and FA were determined in conformity with ASTM C204 [25]. The specific gravity test was carried out to determine the weight per unit volume of the CAC and FA particles according to ASTM C188 [26]. The chemical composition and physical properties of CAC and FA are presented in Table 2.

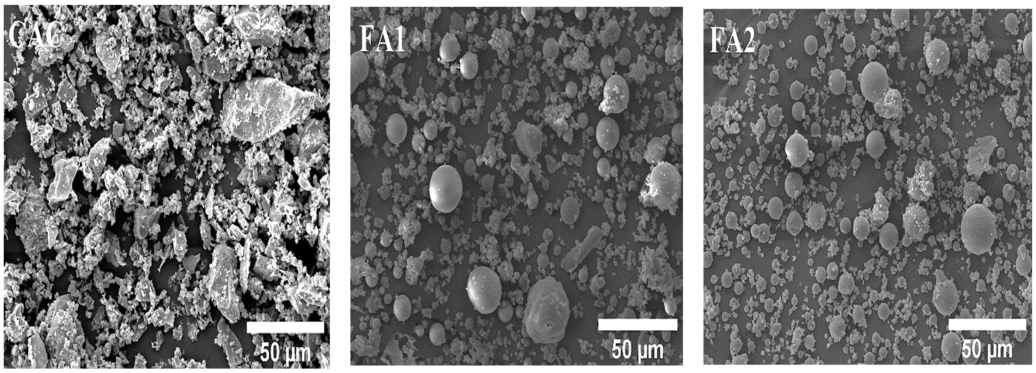

Figure 2. SEM micrographs of CAC, FA1, and FA2.

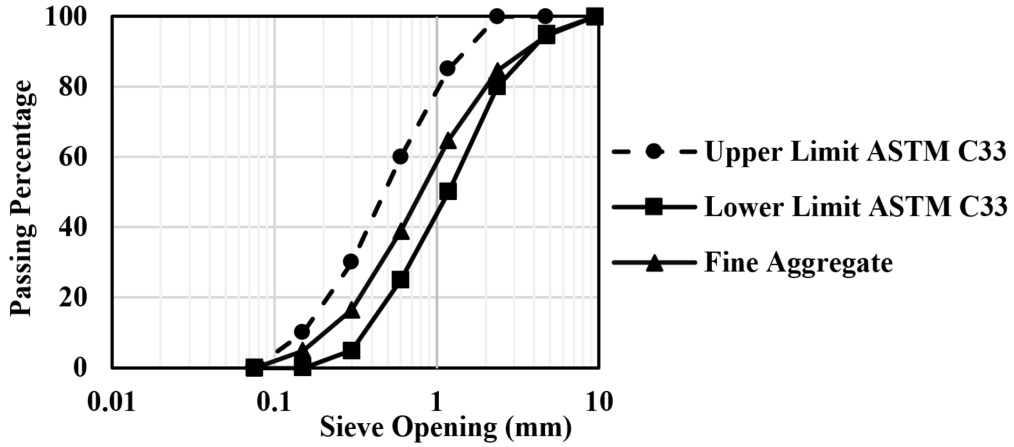

Figure 3. Sieve analysis of fine aggregate.

Table 2. Chemical composition and physical properties of CAC and different FA.

Composition (%)	CAC	FA1	FA2
SiO_2	0.19	73.80	27.40
Al_2O_3	68.9	17.70	15.80
Fe_2O_3	0.13	1.94	12.10
CaO	29.6	0.80	21.60
MgO	0.21	0.31	2.26
SO_3	4.14	0.19	6.92
Na_2O	0.33	0.39	1.70
$SiO_2 + Al_2O_3 + Fe_2O_3$	-	93.44	55.30
LOI	0.5	1.8	0.2
Grade/Class	High alumina	Class F	Class C
Color	White	Gray	Tan
Specific gravity	3.21	2.11	2.40
Blaine surface area (cm^2/g)	3889	4654	4131
Average particle size (μm)	15.6	7.32	7.64

2.2. Preparation of Samples

All mortar mixes produced with two types of FA, namely, FA1M (silica-rich FA) and FA2M (calcium-rich FA), have a 20% replacement level by weight with a binder-sand ratio of 1:2.75 by weight (per ASTM C109) [27] and a water-to-binder ratio (w/b) value of 0.55. Based on previous research [13], a FA substitution level was used as the optimal replacement level for cement. Therefore, this substitution level was selected in the research, as it is a well-established and commonly used substitution level in the industry.

The mortar mix design is given in Table 3. The required amount of water was immediately poured after mixing the materials homogenously in a mechanical mixer. The mortar specimens containing FA were produced according to ASTM C305 [28]. The mixing continued until a uniform mixture was obtained. After the end of mixing, the workability of the fresh mortars was analyzed using the flow table test according to ASTM C1437 [28]. The fresh mixtures were then placed lightly in oiled plastic cubic molds with a dimension of 50 mm for testing the density, compressive strength, and porosity [29]. To maintain the moisture loss, cast specimens were covered with a polyethylene film. After 24 h, the cured specimens were demolded and kept in a water-curing tank at ambient temperature until the designated test age [30]. The SEM/EDS (JSM-IT300LV instrument, JEOL Ltd., Tokyo,

Japan) was used to investigate the morphology of the microstructure, pore structure, and chemical composition of the samples. In addition, the EDS analysis was semi-quantitatively conducted to determine the elemental components.

Table 3. Proportions of mortar mixtures (in kg/m^3).

Mix	CAC	FA	Sand	Water	w/b
CACM	525.00	0.00	1443.75	288.75	0.55
FA1M	420.00	105.00	1443.75	288.75	0.55
FA2M	420.00	105.00	1443.75	288.75	0.55

2.3. Experimental Methods

The initial setting times of CAC pastes (CACP) with different compositions of FA were investigated according to the ASTM C191 standard [31]. Various curing temperatures (30, 40, 60, and 80 °C) were applied to evaluate the reactivity of FA. These curing temperatures were selected based on a combination of factors, including the specific properties of CAC and FA phases, the intended application of the samples, and previous research performed in the field. These curing temperatures were selected to simulate a range of practical conditions. At lower temperatures (30 and 40 °C), the intent was to replicate conditions where the material might experience milder curing environments, such as ambient temperature curing in certain applications. As the temperature increases to 60 and 80 °C, the focus shifts towards investigating the material's behavior under more accelerated curing conditions, which can be relevant for time-sensitive applications. The higher temperatures were selected to assess how the material's properties evolve as exposed to elevated temperature conditions. The observed temperature gradient inconsistencies may arise from complex interactions between the cement and FA phases, heat distribution, and reaction kinetics. In addition, to assess the reactivity of cement paste systems containing class F FA (FA1P) and class C FA (FA2P), the experiment was applied thermodynamically using the Arrhenius Equation as follows:

$$k = k_0 \ \exp(-E_a/RT) \tag{5}$$

where k is the rate coefficient (s^{-1}), k_0 is the pre-exponential constant (s^{-1}); E_a is the activation energy ($J{\cdot}mol^{-1}$), R is the gas constant (=8.314 $J{\cdot}K^{-1}{\cdot}mol^{-1}$), and T is the temperature (K).

Additionally, dry densities of CAC mortars containing different FA at the curing ages of 7, 28, and 56 days have been examined, per ASTM C642 [32]. The cast mortars were made in 50 × 50 × 50 mm^3 cube molds. The measured densities were conducted based on three tests.

The 7-, 28-, and 56-day compressive strengths of CAC mortars containing FA (CACM) were carried out according to ASTM C109/C109M [27]. After casting, mortar specimens were kept in molds at an ambient temperature of 23 ± 2 °C and saturated relative humidity (≥95% RH) for 24 h and then demolded. Demolded specimens were kept in a curing tank until the designated test age. The variety of 7, 28, and 56-day durations is based on industry standards and common practices for assessing the long-term performance of construction materials, including CAC-based materials. These test durations evaluate both early-age properties and the material's evolution over time. The 7-day compressive strength insights into early-age properties are particularly relevant for early strength development. The 28-day compressive strength assesses the material's performance at a more intermediate stage, while the 56-day compressive strength provides insights into the longer-term behavior and durability of the CAC-FA mixtures.

This study considered the porosity and density of CAC mortars affected by the conversion reaction. As mentioned above, the porosity of a cement system is determined by its vital microstructural performances relating to its durability. To determine the porosity of CAC containing FA, their hardened porosity is determined by evaluating the total weight of water in the SSD samples, which have a dimension of 50 × 50 × 50 mm^3. The cubed

specimens were cast and then cured for 7, 28, and 56 days. After that, the specimens were placed in an oven at 105 °C for 24 h, the dried specimens were kept in a water tank to completely penetrate water into their voids. It is noted that at a temperature of 105 °C, all the physically bound and capillary water in the cement paste had completely evaporated. A weight scale with an accuracy of 0.01 g was used to measure the mass of saturated and dried samples. The three specimens were carried out for each test, and the average data and error bars were presented. A similar method was utilized in previous studies by Shen et al. [29]. Equation (6) was determined for calculating the porosity values.

$$p = \frac{M_w - M_d}{v \times \rho} \quad (6)$$

where p is the porosity in %, M_w is the weight of the saturated sample in g, M_d is the weight of the dried sample in g, v is the volume of the sample in cm^3, and ρ is the density of water at 20°C in g/cm^3.

The Brunauer-Emmet-Teller (BET) isotherm is a promising method for assessing the surface area and adsorption properties of a variety of materials [33]. The results obtained from BET analysis can reveal the pore characteristics of CAC-FA composites, which are closely linked to their strengths. In this approach, the sample was tested in vacuum conditions, causing the cement matrix to absorb nitrogen gas using a nitrogen adsorption measurement instrument (Micromeritics 3Flex, Micromeritics Instrument Corporation, Boulder, CO, USA). The quantity of adsorbed nitrogen gas was then quantified to express the surface properties and adsorption capabilities. Using the BET theory, the pore structures of CAC composites ranging from 1 to 500 nm were evaluated. The results presented are the specific surface area and pore volume of the CAC composites.

In addition, powdered specimens cured for 56 days were obtained by extracting material from the central portion of the samples. TGA was carried out using the Perkin Elmer Pyris 1 instrument (PerkinElmer, Shelton, CT, USA) to quantify the extent of CAC conversion. In the TGA procedure, the temperature was incrementally increased from 25 to 1000 °C at a controlled rate of 10 °C per minute while maintaining a continuous nitrogen flow of 70 mL/min. The content of C_3AH_6 was calculated and reported.

For SEM-EDS analysis, the CAC composite's microstructural arrangement was examined. A fracture of hardened CAC was carefully procured, dehydrated, purified, and coated with a layer of gold before being fixed to copper mounts using carbon tape. The SUPRA 66VP ultra-high-resolution equipment(Carl Zeiss AG, Aalen, Germany) was utilized for analyzing the surface morphology and chemical composition of the samples at the microscale.

3. Results

3.1. Chemical Composition of CAC and FA

The chemical compositions of CAC, FA1, and FA2 are illustrated in Table 2. As observed, the principal constituents of CAC are Al_2O_3 > CaO > SiO_2. FA1 and FA2 were largely made up of 73.8% and 27.4% SiO_2, respectively, with other components of Al_2O_3 and CaO. In addition, the CaO content of FA2 (21.6%) was 27 times higher than that of FA1 (0.8%). The silica composition in FA was considered to have pozzolanic properties.

3.2. Initial Setting Time

Figure 4 shows the effect of replacing CAC with a different FA on their initial setting times. Results indicated that the initial setting time of CACP was longer than FA1P and FA2P set at ambient temperature. FA significantly changed the setting time of the CAC. Bensted [2] reported that CAC was moderately gradual stiffening; however, rapid hardening occurred thereafter. Therefore, CAC can provide slow stiffening characteristics at a suitable time for concrete placement without using any retarders. The beginning of steady development of hydrates can also permit this characteristic with a load of time, which enables high early strength development. The results also indicated that control and

CAC binders with silica-rich FA had longer setting times than those with Ca-rich FA for all temperature levels tested at 30, 40, 50, and 60 °C. However, the setting time of CAC without FA noticeably declined at elevated temperatures. Additionally, the process of solidification has been significantly improved by the partial replacement of CAC with FA. The tested results apparently showed that CAC with FA could significantly reduce the setting time, representing accelerated hydration.

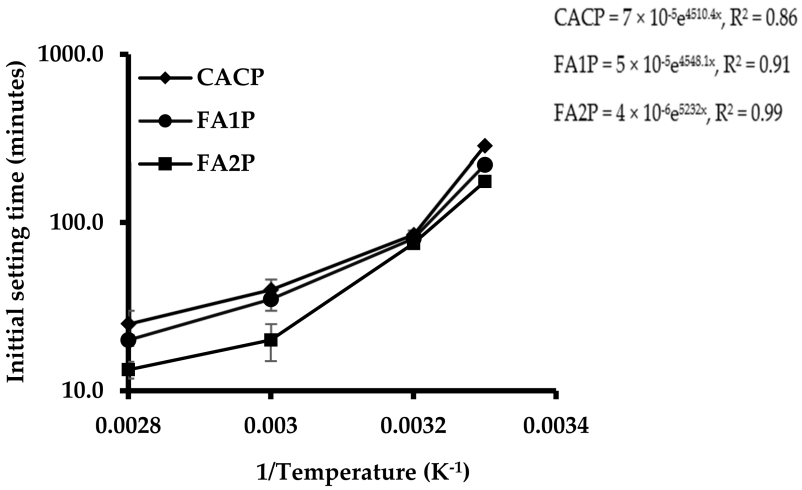

Figure 4. Plot of the effect of FA on the initial setting times of CAC systems (minutes in log scale) as a function of 1/temperature (K^{-1}) and fitted Arrhenius equations (right).

3.3. Assessment of the Reactivity of FA

The Arrhenius equation, which can be used to calculate FA reactivity, is given in Equation (5) and is measured by the initial setting times of the pastes [34]. The activation energy can be denoted by the slope of a straight line. The energy during the stiffening stage is represented as the activation energy, which is calculated here from the initial setting time of CAC paste containing various FA. To change the phase from liquid to solid, higher slopes are associated with a higher activation energy requirement [34]. Temperature is represented as an inverse function of the initial setting time, as illustrated in Figure 4. The findings revealed that the CACP had a steeper slope than the CAC paste with various FAs. This indicated that the CAC paste with FA demanded less energy for paste stiffening than the CAC system. The CAC had more reactive components that rapidly and well reacted with water, leading to a higher rate of heat release and requiring more energy for hydration. In contrast, FA slowly reacted with $Ca(OH)_2$, gradually releasing heat and requiring less energy for hydration.

Therefore, the partial replacement of CAC by FA was used in the conversion reactions of CAC due to the lower consumption of energy. Furthermore, the FA1P had a lower reactivity value than the FA2P, around 13%. Meaningfully, using high-calcium-content FA or class C FA can offer faster reactivity than low-calcium-content FA or class F FA. This contributes to calcium reacting faster than silica at an early age. Although silica offers siliceous reactions at later ages, this should be discussed in Section 3.6.

3.4. Flowability

The flowability test was conducted on fresh mortars per ASTM C1437. Figure 5 demonstrates the workability value of CAC mortar with and without 20% FA. Results revealed that the flow values of all mixes ranged from 76 to 102%. The incorporation of FA in the CAC system led to an increase in flow value. This is generally due to the unique spherical shape of FA particles, which can enhance the workability of concrete by filling in voids between cement particles and lubricating the mixture. Their spherical shape creates a ball-bearing effect, allowing them to move more freely within the mixture, reducing

the friction between particles and improving the flowability of the concrete. This led to a reduction in the amount of water needed to achieve the desired workability.

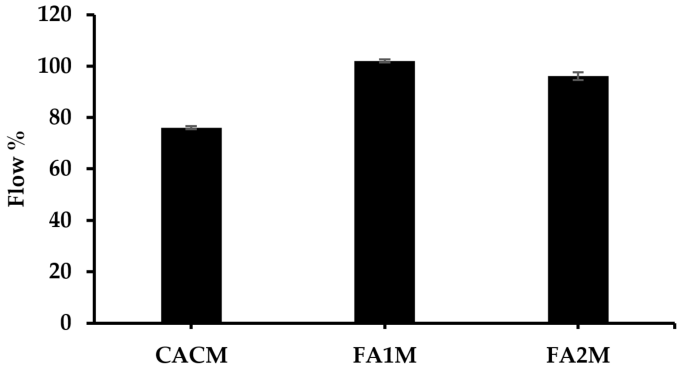

Figure 5. Flow value of fresh CACM with different FA.

The FA1M had the largest flow value of 102 mm, while the CACM exhibited the lowest flow value of 76 mm. The flow of FA2M was approximately 5% lower than FA1M. These FA-based mixes had higher cohesiveness than the control mix. This cohesiveness diminishes segregation all through the mixing, transporting, placing, and compacting processes [35].

3.5. Dry Density

Measuring the densities of mortars is similarly vital as porosity due to their effectiveness in filling gaps in pastes with solid cement components [36]. The plot of the dry density of CACM containing FA for different ages is illustrated in Figure 6. Results exhibited that the dry densities of the CACM samples ranged from 2.34 to 2.42 g/cm^3. The density of CACM cured for 7 days was about 3% higher than that of CACM cured for 28 and 56 days. Moreover, the 7-day densities of these samples were 5% and 9% greater than those containing FA (FA1M and FA2M, respectively). Because FA had a lower specific gravity than CAC, the dry density of the specimens with FA declined. Moreover, the sample density decreased slightly for FA1M. It is implied that the specific gravity of FA1 was smaller than that of CAC and FA2. As a result, the 28- and 56-day densities of CACM without FA had the lowest density values, while the 28- and 56-day densities of FA2M had the highest values. This was because their densities were different, with conversion phases leading to the development of porosity (which will be discussed in Section 3.7). The densities of intermediate phases CA and C_2AH_8 are 2.98 and 1.97, respectively, whereas the converted phases C_3AH_6 and AH_3 are 2.52 and 2.44 [2]. For that reason, the conversion of the CAC hydrates to C_3AH_6 and AH_3 permitted porosity enhancement. Moreover, the formation of density is consistent with the mechanical properties of CACM, including FA.

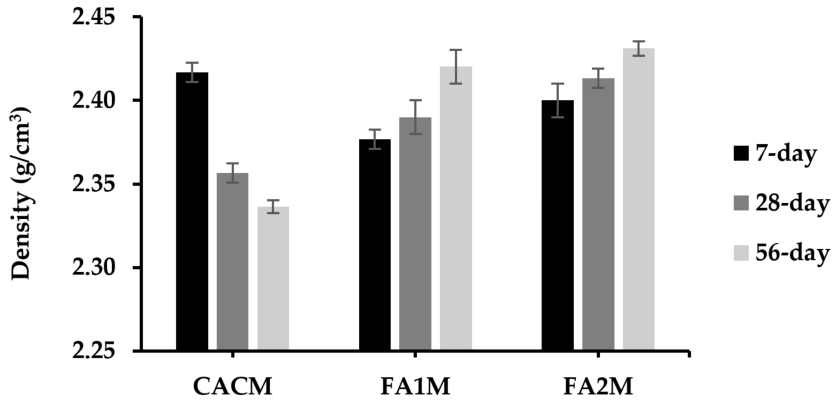

Figure 6. Dry density of CACM with different types of FA cured for 7, 28, and 56 days.

3.6. Compressive Strength

Figure 7 shows 7-, 28-, and 56-day mortar compressive strengths having FA. The 7-, 28-, and 56-day compressive strengths of CACM were 28.3, 24.6, and 22.9 MPa, respectively. According to the observed results, the 7-day compressive strengths of the CACM were 15% and 24% higher than those of the CACM cured for 28 and 56 days, respectively. Moreover, the 7-day compressive strength of the CACM was 30% and 11.5% higher than the FA1M and FA2M. The strength improvement of CAC concrete at ambient temperature has the phase formations illustrated in Figure 1 [16], with an initial improvement sharply increasing to an elevated early strength (corresponding to CAH_{10} and C_2AH_8).

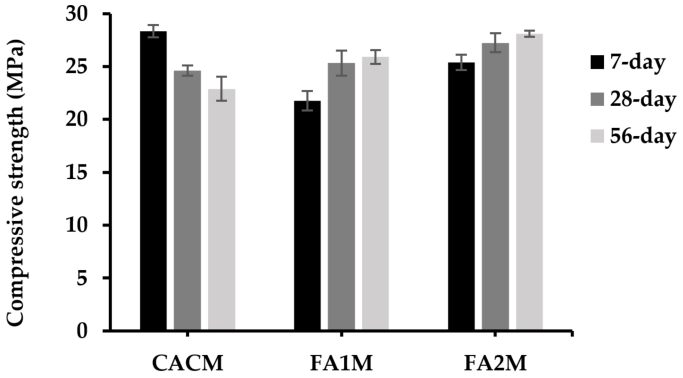

Figure 7. Compressive strengths of CACM containing different FA cured for 7, 28, and 56 days.

Conversely, the presence of FA in the CAC system offers higher 28- and 56-day compressive strengths when compared to the control. Previous studies [37,38] investigated a similar figure and considered that one of the key factors determining the compressive strength and durability of the FA-cement system was the pozzolanic reactivity. Additionally, results found that pozzolanic materials with larger silica contents reacted with $Ca(OH)_2$ more readily and thus produced C–(A)–S–H at higher contents. The chemical and physical effects of FA determined their compressive strength development. The pozzolanic reactions between the amorphous silica in FA and $Ca(OH)_2$, which were produced by the hydration reaction of cement to create C–S–H gel, were mostly responsible for the chemical effect. The physical effect, known as the "filler effect," was that FA particles improved the packing of solid materials by filling the spaces between the cement grains, similarly to how the cement particles filled the spaces between fine aggregate particles.

In addition, FA2M led to one of the highest compressive strength developments (25.91 and 28.76 MPa) in CAC-FA systems in both 28- and 56-day compressive strengths. Results found that there were 5% and 8.5% greater compressive strengths of the FA2M compared with the FA1M at 28- and 56-day curing periods, respectively. Although the compressive strength of FA2M was greater than that of FA1M at all testing ages, the trend was likely to be the same in both FA1M and FA2M. As the CAC was replaced by FA2, the compressive strength increased to lesser extents, which was likely because of the high silica content in FA2 that was assessable with $Ca(OH)_2$ formed from the hydrate reaction. It was reported that once the cement systems contained huge amounts of silica during hydration, because they could not release enough $Ca(OH)_2$ to hydrate with all the available silica, some silica remained present without causing any chemical reaction [39]. Later, a substantial portion of silica was absent from the chemical reactions [39].

In addition, after 7 days of curing, the conversion of all CACM occurred, which resulted in a suddenly reduced compressive strength. It is inferred due to the conversion of CAC. Nonetheless, using FA in CAC diminished the conversion process from metastable phases (CAH_{10} and C_2AH_8) to stable phases (C_3AH_6 and AH_3). It can be explained that the C_2ASH_8 development in the case of loss of compressive strength could be lessened if there was FA content. By generating a favorable situation for the creation of C_2ASH_8 instead of C_3AH_6 by inducing calcium ions in the pore solution to be consumed, the insertion of FA

in this work was seen to prevent the phase evolution to a calcium-rich phase, C_3AH_6 [20]. It is noticeable that at room temperature, the primary hydrates of CAC having siliceous materials have been described to form as C_3AH_{10}, C_2AH_8, C-(A)-S-H, and AH_3 gel phases. Therefore, this resulted in a decrease in mechanical strength since the phase shift in CAC accompanied an increase in porosity in a rigid state [40,41]. This phenomenon is detailed in Section 3.7.

3.7. Porosity

Porosity is a crucial factor influencing the strength, durability, and mechanical effectiveness of concrete. The porosity of the hydrated CACM increased, as shown in Figure 8. As a result, the 7-day porosity of CACM was 13% and 19% lower than the CACM at 28- and 56-day curing ages, where the values ranged between 12.1% and 15.0%. In addition, the porosity of the CACM cured for 7 days was about 19% and 5% lower than the FA1M and FA2M. On the other hand, the 28- and 56-day porosities of CACM were significantly higher than FA1M and FA2M. Therefore, replacing CAC with FA resulted in reduced porosity by approximately 8% to 48% at longer curing ages. The figures of FA1M and FA2M exhibited lower porosity values in the CAC-FA systems over time, whereas the conversion took place in CACM at longer ages. It was apparently seen that FA2M stood as one of the lowest porosity values (11.23% and 7.8%) at both 28 and 56 days, respectively. Since the pozzolanic reaction of FA reacts for a longer time, called the second reaction, the FA cannot provide a satisfactory reaction for the first 7 days. Based on the results, the converted CACM increases porosity considerably when compared to FA1M and FA2M. This indicates that conversion significantly influences the morphology of CAC.

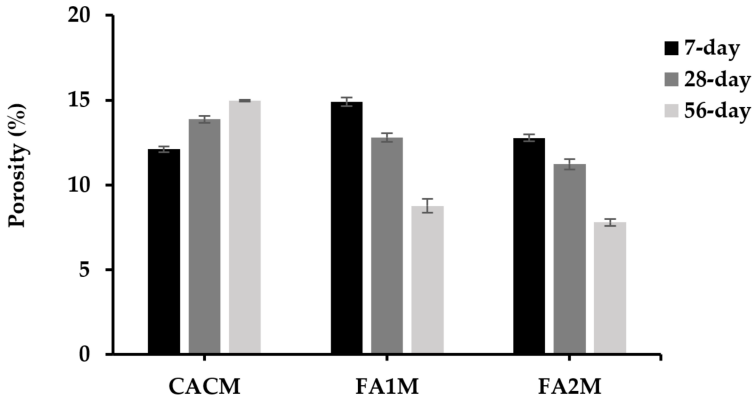

Figure 8. Porosity of CACM with different FA cured for 7, 28, and 56 days.

Bensted [2] suggested that the increase in porosity could be attributed to the formation effects resulting from conversion processes. This was observed due to the higher density found in the converted phase (C_3AH_6) compared to the metastable phase. While the formation of stable C_3AH_6 and AH_3 increased porosity in the CAC conversion, which allowed for strength reduction. The formation of metastable phases resisted and controlled the shrinkage of the hydrated CAC [42]. There will be a higher ingress of CAC with more porosity, which will worsen its durability. According to Equations (1) and (2), the aforementioned conversion reactions cause CAC to become more porous, permeable, and weaker as a result of the release of water from the conversion structure and the production of a packed C_3AH_6 (which results in a reduction in the molar volume of the solids) [43,44].

3.8. BET Isotherm Analysis

The nitrogen sorption isotherms for all mixtures are shown in Figure 9. During the early phases of sorption (at p/p° values between 0 and 0.1), there is rapid initial molecular coverage on the surfaces of the pores as the gas pressure rises. Subsequently, the rate of sorption volume increase diminishes considerably, resulting in a distinct bend known as

a 'knee' [45]. The knee characteristics are essential for distinguishing between monolayer and multilayer sorption. Less overlap exists between monolayer coverage and the start of multilayer adsorption if the curvature is more pronounced (indicating a more distinct turning point). The isotherms show that during the initial sorption phase, all of the knees have very strong, clearly defined turning points (shown by the arrow in Figure 9). This means that the sorption is changing from monolayer coverage to multilayer. As the relative gas pressure rises to 0.7, the adsorption volume increases gradually and progressively. The IU-PAC type II pattern [45] is approximately followed by the adsorption branches of the isotherms, indicating that the tested materials possess macropores. When the relative gas pressure drops from 1 (0.98 in actual testing) to 0.45, the desorption and adsorption branches move away from each other. This causes hysteresis loops to form in this range of gas pressure (p/p° between 0.45 and 1). According to IUPAC standards [45], these hysteresis loops are of the H3 type, which can be attributed to the presence of macro-porous structures. Notably, the hysteresis loop observed in the CACP sample was slightly larger than that observed in the other samples, presumably due to the CAC system's conversion process. The FA1P and FA2P mixtures exhibited comparable isotherm geometries and hysteresis loops, indicating that their pore structures can be comparable.

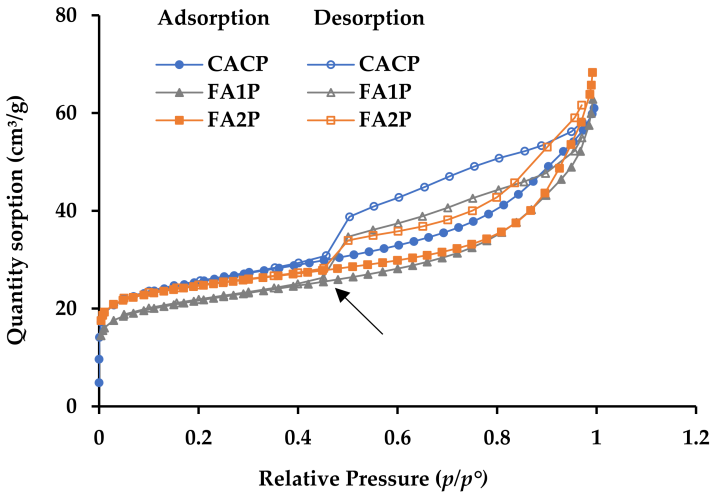

Figure 9. Nitrogen sorption isotherms of all mixes.

Furthermore, the hysteresis loops observed in the FA1P and FA2P gradually diminished in size and became less prominent when compared to the hysteresis loop of the CACP, which primarily occurred at higher pressures ($p/p^{\circ} > 0.6$). This observation suggests a decrease in the porosity of the FA1P and FA2P, indicating smaller pore volumes compared to the CACP, where its pronounced hysteresis loop is evident. This phenomenon can be attributed to the limited number of pores introduced by the incorporation of FA. Consequently, the conversion process of CAC containing FA resulted in lower strength loss when compared to CACP, as detailed in Table 4. The analysis revealed that the surface area of CACP was notably higher than that of FA1P and FA2P. As a result, the inclusion of FA led to a reduction in surface area. Regarding total pore volume, the findings showed that incorporating FA2P into the CAC system resulted in an 8.4% reduction as compared with CACP. The incorporation of FA effectively promotes the development of CAC composites with finer pore structures.

Table 4. Pore structure of CAC composites containing different FA.

	CACP	FA1P	FA2P
Surface area (m^2/g)	82.824	78.666	70.633
Total pore volume (cm^3/g)	0.083	0.077	0.076

3.9. TGA

Figure 10 presents the TGA analyses of hydrated CAC systems containing FA. As shown in Equations (7)–(10), when a heated sample of hydrated CAC breaks down, chemically bound water is released from its different aluminate hydrates. This investigation reveals that AH_3 releases the bound water at 250 °C, and the C_3AH_6 phase releases the bound water at 300 °C. These findings can also be found elsewhere [20,46–48].

$$CAH_{10} \longrightarrow CaAl_2O_4 + 10H_2O \text{ (100–160 °C)} \quad (7)$$

$$C_2AH_8 \longrightarrow Ca_2Al_2O_5 + 8H_2O \text{ (140–200 °C)} \quad (8)$$

$$AH_3 \longrightarrow Al_2O_3 + 3H_2O \text{ (210–300 °C)} \quad (9)$$

$$C_3AH_6 \longrightarrow Ca_3Al_2O_6 + 6H_2O \text{ (240–370 °C)} \quad (10)$$

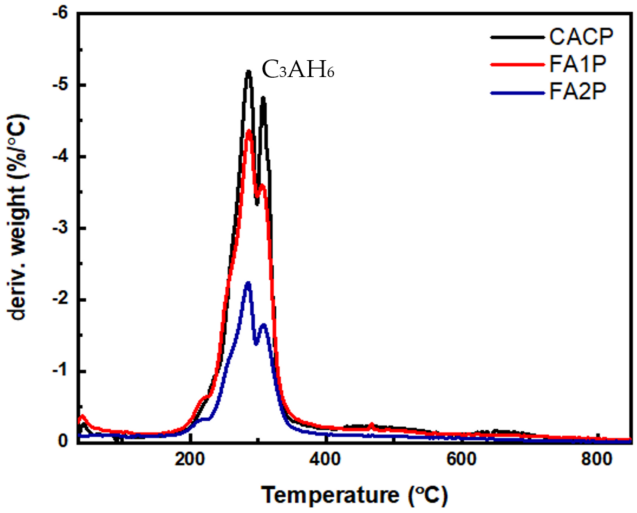

Figure 10. The DTG curve of CAC composites including FA.

The results showed that TGA analysis only found AH_3 and C_3AH_6 hydrates. There were no signs of additional CAH_{10} or C_2AH_8 phases in the samples. The reason behind this absence is that a significant portion of the C_2AH_8 transformed into AH_3 and C_3AH_6. These results are consistent with prior research findings regarding the transformation of metastable phases into C_3AH_6. Equation (11) was used to determine the quantity of C_3AH_6.

$$C_3AH_6 = WL_{C_3AH_6} \times \frac{m_{C_3AH_6}}{6 \times m_{H_2O}} \quad (11)$$

where C_3AH_6 is the amount of measured C_3AH_6 present in the mixture (%), and WL_{C3AH6} is the weight loss percentage due to water evaporation within the range of 240 to 370 °C. Moreover, m_{C3AH6} is the molecular weight of C_3AH_6 (378 g/mol), and m_{H2O} is the molecular weight of water (18 g/mol). The outcomes are given in Table 5, illustrating the calculated percentages of transformed C_3AH_6 within the CAC system. Obviously, CACP yields a notable expansion in the corresponding area, indicating heightened conversion and a greater presence of C_3AH_6. Conversely, when employing FA, notably FA2P, the formation of C_3AH_6 is reduced. This can be attributed to the CASH phase formation of FA1P and FA2P.

Table 5. Percentage of C_3AH_6 of CAC containing FA from TGA analysis.

	CACP	FA1P	FA2P
C_3AH_6 (%)	57.7	45.7	44.1

3.10. Microstructure Assessment

SEM micrographs of CAC/FA specimens are illustrated in Figure 11. Some of the pores caused by the conversion hydration in CACP were very obvious, and due to the lack of FA, the highly porous structure of the CACP was obvious. Moreover, there was a larger size and number of pores in CACP compared with FA1P and FA2P. The larger size and increased number of pores can result in the mechanical properties of CAC deteriorating. In contrast, CAC containing FA1 and FA2 showed a more uniform and compact microstructure in the cement matrix. In addition, while comparing the micrographs of both FA1P and FA2P samples, it became obvious that FA2P had a denser and lower inter-particle space than FA1P. It is evident that by replacing FA2 in CAC, the surface of these samples' morphology showed a radical transition from a non-compact, porous structure to a compact one. This could also happen because FA1 has a larger specific surface area than FA2 and CAC, resulting in a higher rate of hydration due to its high pozzolanic reactivity. According to some researchers [49,50], the replacement of pozzolans has also led to an improvement in the mechanical properties of concrete. Chousidis et al. [51] observed that the reinforced concrete structure containing FA improved compressive strength and decreased porosity.

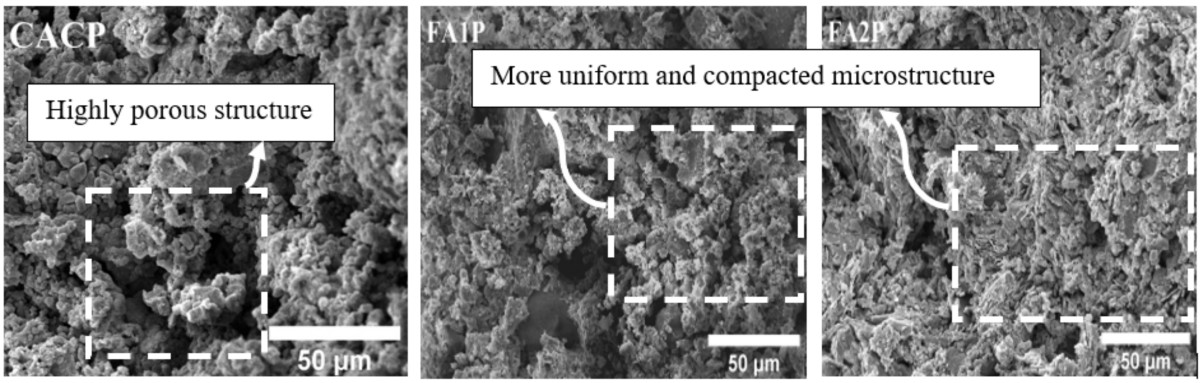

Figure 11. SEM micrographs of CACP, FA1P, and FA2P.

4. Discussion

As aforementioned, the performance of FA in CAC systems is strongly influenced by its physical and chemical properties. The ternary diagram of CAC systems containing different FAs is depicted in Figure 12. Regarding the early-age properties, different activation energies of CAC systems with FA contribute to calcium reacting faster than silica at a very young age. Different FAs can offer different [52] activities. These reactions thereafter change hydration reactions. When CAC mortar is converted, it undergoes a process of mineralogical development, and the porosity has increased. Therefore, the conversion method could avoid the reaction that could be formed in the subsequent way [2,3,10,11,44]. The mineral admixtures containing silica would react first with the CA, avoiding the formation of C_2AH_8 and, subsequently, the conversion into C_3AH_6. Consequently, instead of this C_3AH_6 phase, the C_2ASH_8 phase was proposed to be formed. This implies that samples containing FA exhibit reduced levels of stable phases and encounter comparatively lesser degrees of strength loss (see Table 5).

Based on SEM-EDS images as shown in Figure 13 and Table 6 of CAC specimens prepared from fractured surfaces after 56-day water curing, The main elements involve Al, Si, and Ca, and other elements C and O. By using FA, a pozzolan with a high specific surface area and strong reactivity, in relation to the CACP sample, the concentration of the remaining $Ca(OH)_2$ and silicon dioxide (SiO_2) among the compounds was reduced, according to data from EDS elemental compositions for each system. This showed that these components had a higher likelihood of forming C-(A)-S-H gel when FA was present in the specimens, which consequently improved the strength and decreased porosity. It is believed that, compared to the control sample, CAC specimens containing FA exhibit enhanced mechanical characteristics. In addition, it is likely that the specimen lacking FA

will perform poorly in terms of mechanical properties given the quantity and size of pores among the samples in this work.

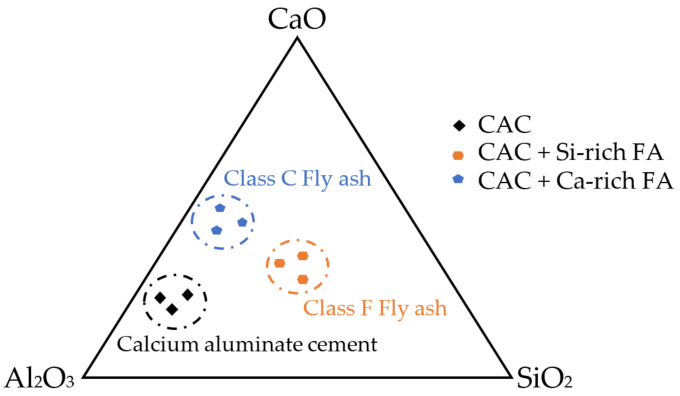

Figure 12. Ternary diagram of CAC, CAC + Ca-rich FA, and CAC + Si-rich FA.

The partial utilization of FA in CAC systems, especially for class-C FA, improved the quality of resultant products from very early to later ages. It can be mainly adopted for increasing sustainability in our manufacturing industries such as construction, refractory, and rapid repair applications, as well as reducing material costs since FA is an industrial by-product that is less expensive, and using it can increase reactivity so that the CAC can be used in smaller fractions.

In summary, the incorporation of FA into CAC offers numerous advantages, including improved environmental sustainability and enhanced material performance. By introducing FA into CAC, we contribute to the cement industry's efforts to combat climate change. Our study has shown that FA addition leads to a range of beneficial effects on CAC properties. Firstly, it results in a reduced setting time, enhancing construction efficiency and reducing construction time. Additionally, FA improves workability and positively influences microstructural characteristics. This includes the increased formation of C-(A)-S-H phases and the reduction of inter-particle space, indicating the pozzolanic action of FA. These changes lead to improved microstructure, density, and compressive strength, which are highly desirable attributes in the construction industry. Furthermore, the presence of FA in CAC alters the kinetics of hydration reactions, lowering the activation energy required for the conversion process. This has significant implications for the material's setting time, strength development, and overall performance. While our study highlights the positive impacts of FA on CAC, further research is needed to fully understand the mechanisms underlying FAs' influence on the conversion process of CAC. This will enable us to optimize the use of FA for specific applications in the construction industry, ultimately advancing both environmental sustainability and construction practices.

Table 6. EDS elemental composition (mass%) shown in SEM micrographs.

Sample	Element	C	O	Al	Si	Ca
CACM	Wt. %	-	52.46	23.25	-	24.28
	At. %	-	69.08	18.16	-	12.76
FA1M	Wt. %	4.25	49.53	22.43	3.35	20.44
	At. %	7.21	63.05	16.93	2.43	10.39
FA2M	Wt. %	-	53.36	28.16	-	18.49
	At. %	-	68.91	21.56	-	9.53

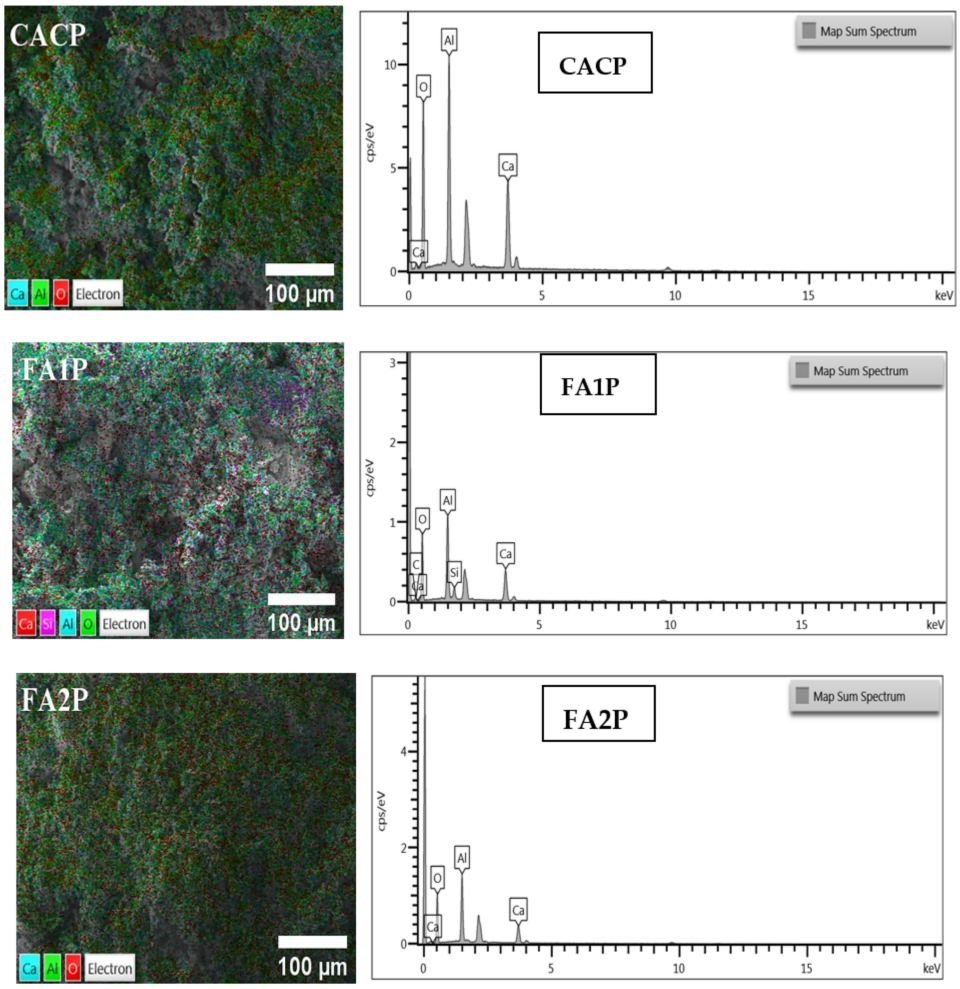

Figure 13. SEM micrographs (**left**) and EDS elemental spectra (**right**) of CACP, FA1P, and FA2P after 56-day water curing.

5. Conclusions

This work examined the utilization of different compositions of FA affecting the conversion of CAC. When the CAC materials considered in this research were mixed with FA, the conclusions were made as follows:

- CAC with fly ash can be satisfied by minimizing its conversion process.
- Adding FA resulted in a reduction in setting time and thus reduced the required activation energy contributed by the decrease in the slope of the FA-CAC system. Therefore, FA could be utilized to improve the hydration of CAC.
- CAC containing FA influenced the fresh properties through increasing workability. This behavior was due to the high surface area and spherical shape of the particles, and thus the high reactivity of FA particles with $Ca(OH)_2$.
- Increased gel formation C-(A)-S-H, reduced inter-particle space, and lowered porous surfaces were found in the microstructural CAC containing FA. This resulted in improved microstructure, density, and compressive strength due to the pozzolanic action.
- Utilizing FA in the BET test resulted in alterations to the pore structure, yielding a matrix characterized by reduced mesopore volume.
- TGA analysis revealed that when FA was presented, the mitigation of CAC conversion and the yield of the lower stable C_3AH_6 phase were seen.
- CAC with calcium-rich FA resulted in denser and lower mesopores than the silica-rich FA, leading to higher compressive strength. This is caused by the larger CaO formation.

These findings investigate that replacing the CAC with FA not only promotes cost efficiency but also paves the way for environmentally friendly, sustainable development. Additionally, this method reduces greenhouse gas emissions that the cement industry releases into the atmosphere, which is advantageous for preventing climate change. The effects of FA on CAC with different chemical compositions and different micropore structures on both early- and later-age performance should be further investigated. Other by-products containing a high calcium content should also be assessed.

Author Contributions: Conceptualization, L.P.; methodology, T.T.W. and L.P.; investigation, T.T.W.; writing—original draft preparation, T.T.W.; writing—review and editing, C.P., P.J., W.P. and L.P.; visualization, L.P.; supervision, L.P.; project administration, L.P., P.J. and W.P.; funding acquisition, L.P. All authors have read and agreed to the published version of the manuscript.

Funding: This project is funded by the National Research Council of Thailand (NRCT) and Chulalongkorn University (Grant No. N42A660629). This research is also funded by the Thailand Science Research and Innovation Fund at Chulalongkorn University (SOC66250010).

Data Availability Statement: Some or all data, models, or code that support the findings of this study are available from the corresponding author upon reasonable request.

Acknowledgments: The authors would like to thank Siam Refractory Industry Co., Ltd. for donating the material, "Chulalongkorn Academic Advancement into its Second Century Fund (C2F) for Postdoctoral Fellowship (T.T.W.), Chulalongkorn University, and British Council—Thai-UK World-Class University Consortium 2022".

Conflicts of Interest: The authors report that there are no competing interests to declare.

References

1. Abolhasani, A.; Samali, B.; Aslani, F. Physicochemical, Mineralogical, and Mechanical Properties of Calcium Aluminate Cement Concrete Exposed to Elevated Temperatures. *Materials* **2021**, *14*, 3855. [CrossRef]
2. Bensted, J. Calcium Aluminate Cements. *Struct. Perform. Cem.* **2002**, *2*, 114–138. Available online: https://books.google.co.th/books?hl=en&lr=&id=6wPpkyrWE5oC&oi=fnd&pg=PA114&dq (accessed on 10 March 2022).
3. Zapata, J.F.; Gomez, M.; Colorado, H.A. Cracking in Calcium Aluminate Cement Pastes Induced at Different Exposure Temperatures. *J. Mater. Eng. Perform.* **2019**, *28*, 7502–7513. [CrossRef]
4. Zapata, J.F.; Gomezc, M.; Colorado, H.A. *Characterization of Two Calcium Aluminate Cement Pastes*; John Wiley & Sons: Hoboken, NJ, USA, 2017; Volume 263, pp. 491–503. [CrossRef]
5. Zapata, J.F.; Gomez, M.; Colorado, H.A. Calcium Aluminate Cements Subject to High Temperature. *Adv. Mater. Sci. Environ. Energy Technol. VI* **2017**, *262*, 97. Available online: https://books.google.co.th/books?hl=en&lr=&id=Nlg7DwAAQBAJ&oi=fnd&pg=PA97&dq=Calcium+aluminate+cements+subject+to+high+temperature (accessed on 28 June 2022).
6. Boris, R.; Wilińska, I.; Pacewska, B.; Antonovič, V. Investigations of the Influence of Nano-Admixtures on Early Hydration and Selected Properties of Calcium Aluminate Cement Paste. *Materials* **2022**, *15*, 4958. [CrossRef]
7. Antonovič, V.; Kerienė, J.; Boris, R.; Aleknevičius, M. The Effect of Temperature on the Formation of the Hydrated Calcium Aluminate Cement Structure. *Procedia Eng.* **2013**, *57*, 99–106. [CrossRef]
8. Midgley, H. Quantitative determination of phases in high alumina cement clinkers by X-ray diffraction. *Cem. Concr. Res.* **1976**, *6*, 217–223. [CrossRef]
9. Zapata, J.F.; Colorado, H.A.; Gomez, M.A. Effect of high temperature and additions of silica on the microstructure and properties of calcium aluminate cement pastes. *J. Sustain. Cem. Mater.* **2020**, *9*, 323–349. [CrossRef]
10. López, A.H.; Calvo, J.L.G.; Olmo, J.G.; Petit, S.; Alonso, M.C. Microstructural Evolution of Calcium Aluminate Cements Hydration with Silica Fume and Fly Ash Additions by Scanning Electron Microscopy, and Mid and Near-Infrared Spectroscopy. *J. Am. Ceram. Soc.* **2008**, *91*, 1258–1265. [CrossRef]
11. Majumdar, A.; Singh, B. Properties of some blended high-alumina cements. *Cem. Concr. Res.* **1992**, *22*, 1101–1114. [CrossRef]
12. Cong, X.; Kirkpatrick, R.J. Hydration of Calcium Aluminate Cements: A Solid-State 27 Al NMR Study. *J. Am. Ceram. Soc.* **1993**, *76*, 409–416. [CrossRef]
13. Win, T.T.; Wattanapornprom, R.; Prasittisopin, L.; Pansuk, W.; Pheinsusom, P. Investigation of Fineness and Calcium-Oxide Content in Fly Ash from ASEAN Region on Properties and Durability of Cement–Fly Ash System. *Eng. J.* **2022**, *26*, 77–90. [CrossRef]
14. Vafaei, M.; Allahverdi, A. Influence of calcium aluminate cement on geopolymerization of natural pozzolan. *Constr. Build. Mater.* **2016**, *114*, 290–296. [CrossRef]
15. Abolhasani, A.; Nazarpour, H.; Dehestani, M. The fracture behavior and microstructure of calcium aluminate cement concrete with various water-cement ratios. *Theor. Appl. Fract. Mech.* **2020**, *109*, 102690. [CrossRef]

16. Scrivener, K.L.; Cabiron, J.-L.; Letourneux, R. High-performance concretes from calcium aluminate cements. *Cem. Concr. Res.* **1999**, *29*, 1215–1223. [CrossRef]
17. Adams, M.P.; Ideker, J.H. Influence of aggregate type on conversion and strength in calcium aluminate cement concrete. *Cem. Concr. Res.* **2017**, *100*, 284–296. [CrossRef]
18. Khaliq, W.; Khan, H.A. High temperature material properties of calcium aluminate cement concrete. *Constr. Build. Mater.* **2015**, *94*, 475–487. [CrossRef]
19. Zapata, J.F.; Azevedo, A.; Fontes, C.; Monteiro, S.N.; Colorado, H.A. Environmental Impact and Sustainability of Calcium Aluminate Cements. *Sustainability* **2022**, *14*, 2751. [CrossRef]
20. Son, H.; Park, S.; Jang, J.; Lee, H. Effect of nano-silica on hydration and conversion of calcium aluminate cement. *Constr. Build. Mater.* **2018**, *169*, 819–825. [CrossRef]
21. Ukrainczyk, N.; Matusinović, T. Thermal properties of hydrating calcium aluminate cement pastes. *Cem. Concr. Res.* **2010**, *40*, 128–136. [CrossRef]
22. *ASTM C33-18*; Standard Specification for Concrete Aggregates. American Society of Testing Materials: West Conshohocken, PA, USA, 2018.
23. *ASTM C128-15*; Standard Test Method for Density, Relative Density (Specific Gravity), and Absorption of Fine Aggregate. American Society of Testing Materials: West Conshohocken, PA, USA, 2015.
24. *ASTM C618-19*; Standard Specification for Coal Fly Ash and Raw or Calcined Natural Pozzolan for Use in Concrete. American Society of Testing Materials: West Conshohocken, PA, USA, 2019.
25. *ASTM C204-18*; Standard Test Method for Fineness of Hydraulic Cement by Air-Permeability Apparatus. American Society of Testing Materials: West Conshohocken, PA, USA, 2018.
26. *ASTM C188-17*; Standard Test Method for Density of Hydraulic Cement. American Society of Testing Materials: West Conshohocken, PA, USA, 2017.
27. *ASTM C109/C109M-16*; Standard Test Method for Compressive Strength of Hydraulic Cement Mortars (Using 2-in. or [50-mm] Cube Specimens). American Society of Testing Materials: West Conshohocken, PA, USA, 2016.
28. *ASTM C1437-20*; Standard Test Method for Flow of Hydraulic Cement Mortar. American Society of Testing Materials: West Conshohocken, PA, USA, 2020.
29. Shen, J.; Xu, Q. Effect of moisture content and porosity on compressive strength of concrete during drying at 105 °C. *Constr. Build. Mater.* **2018**, *195*, 19–27. [CrossRef]
30. *ASTM C511-19*; Standard Specification for Mixing Room; Moist Cabinets; Moist Rooms; and Water Storage Tanks Used in the Testing of Hydraulic Cements and Concretes. American Society of Testing Materials: West Conshohocken, PA, USA, 2019.
31. *ASTM C191-21*; Standard Test Method for Time of Setting of Hydraulic Cement by Vicat Needle. American Society of Testing Materials: West Conshohocken, PA, USA, 2021.
32. *ASTM C642-21*; Standard Test Method for Density, Absorption, and Voids in Hardened Concrete. American Society of Testing Materials: West Conshohocken, PA, USA, 2021.
33. De Belie, N.; Kratky, J.; Van Vlierberghe, S. Influence of pozzolans and slag on the microstructure of partially carbonated cement paste by means of water vapour and nitrogen sorption experiments and BET calculations. *Cem. Concr. Res.* **2010**, *40*, 1723–1733. [CrossRef]
34. Prasittisopin, L.; Sereewatthanawut, I. Effects of seeding nucleation agent on geopolymerization process of fly-ash geopolymer. *Front. Struct. Civ. Eng.* **2017**, *12*, 16–25. [CrossRef]
35. Mehta, P.K.; Monteiro, P.J. *Concrete: Microstructure, Properties, and Materials*; McGraw-Hill: New York, NY, USA, 2014. Available online: https://www.accessengineeringlibrary.com/binary/mheaeworks (accessed on 1 August 2022).
36. Balonis, M.; Glasser, F. The density of cement phases. *Cem. Concr. Res.* **2009**, *39*, 733–739. [CrossRef]
37. Le, H.T.; Ludwig, H.-M. Effect of rice husk ash and other mineral admixtures on properties of self-compacting high performance concrete. *Mater. Des.* **2016**, *89*, 156–166. [CrossRef]
38. Hefni, Y.; El Zaher, Y.A.; Wahab, M.A. Influence of activation of fly ash on the mechanical properties of concrete. *Constr. Build. Mater.* **2018**, *172*, 728–734. [CrossRef]
39. Prasittisopin, L.; Trejo, D. Characterization of Chemical Treatment Method for Rice Husk Ash Cementing Materials. *ACI Symp. Publ.* **2013**, *294*, 1–14. [CrossRef]
40. Park, S.; Jang, J.; Son, H.; Lee, H. Stable conversion of metastable hydrates in calcium aluminate cement by early carbonation curing. *J. CO2 Util.* **2017**, *21*, 224–226. [CrossRef]
41. Juenger, M.; Winnefeld, F.; Provis, J.; Ideker, J. Advances in alternative cementitious binders. *Cem. Concr. Res.* **2011**, *41*, 1232–1243. [CrossRef]
42. Scrivener, K.; Capmas, A. Calcium Aluminate Cements. *Adv. Concr. Technol.* **2003**, 1–31. Available online: https://books.google.co.th/books?hl=en&lr=&id=IMdF-QR_8mkC&oi=fnd&pg=SA2-PA1&dq=Calcium+aluminate+cements (accessed on 12 April 2022).
43. Sio, J.D. Influence of Pozzolanic Material in the Conversion and Corrosion Behaviour of Calcium Aluminate Cement. Master's Thesis, University of Sydney, Camperdown, Australia, 2014. Available online: https://hdl.handle.net/2123/12694 (accessed on 1 August 2022).
44. Sereewatthanawut, I.; Prasittisopin, L. Effects of accelerating and retarding agents on nucleation and crystal growth of calcium aluminate cement. *Open Ceram.* **2022**, *11*, 100290. [CrossRef]

45. Thommes, M.; Kaneko, K.; Neimark, A.V.; Olivier, J.P.; Rodriguez-Reinoso, F.; Rouquerol, J.; Sing, K.S.W. Physisorption of gases, with special reference to the evaluation of surface area and pore size distribution (IUPAC Technical Report). *Pure Appl. Chem.* **2015**, *87*, 1051–1069. [CrossRef]
46. Prasittisopin, L.; Trejo, D. Performance Characteristics of Blended Cementitious Systems Incorporating Chemically Transformed Rice Husk Ash. *Adv. Civ. Eng. Mater.* **2017**, *6*, 17–35. [CrossRef]
47. Ahmed, A.A.; Shakouri, M.; Trejo, D.; Vaddey, N.P. Effect of curing temperature and water-to-cement ratio on corrosion of steel in calcium aluminate cement concrete. *Constr. Build. Mater.* **2022**, *350*, 128875. [CrossRef]
48. Win, T.T.; Prasittisopin, L.; Jongvivatsakul, P.; Likitlersuang, S. Investigating the synergistic effect of graphene nanoplatelets and fly ash on the mechanical properties and microstructure of calcium aluminate cement composites. *J. Build. Eng.* **2023**, *78*, 107710. [CrossRef]
49. Nakamura, K.; Inoue, Y.; Komai, T. Consideration of strength development by three-dimensional visualization of porosity distribution in coal fly ash concrete. *J. Build. Eng.* **2020**, *35*, 101948. [CrossRef]
50. Sereewatthanawut, I.; Panwisawas, C.; Ngamkhanong, C.; Prasittisopin, L. Effects of extended mixing processes on fresh, hardened and durable properties of cement systems incorporating fly ash. *Sci. Rep.* **2023**, *13*, 6091. [CrossRef]
51. Chousidis, N.; Rakanta, E.; Ioannou, I.; Batis, G. Mechanical properties and durability performance of reinforced concrete containing fly ash. *Constr. Build. Mater.* **2015**, *101*, 810–817. [CrossRef]
52. Chopra, D.; Siddique, R.; Kunal. Strength, permeability and microstructure of self-compacting concrete containing rice husk ash. *Biosyst. Eng.* **2015**, *30*, 72–80. [CrossRef]